

ISTITUTO NAZIONALE DI FISICA NUCLEARE
Laboratori Nazionali di Frascati

LNF-82/63(R)

4 Agosto 1982

(Revised Version 4 Marzo 1983)

F. Antonangeli and M. Piacentini:
RAY TRACING CALCULATIONS FOR THE PULS FACILITY
PART I: THE MERIDIAN PLANE

RAY TRACING CALCULATIONS FOR THE PULS FACILITY

PART I: THE MERIDIAN PLANE

F. Antonangeli and M. Piacentini
Gruppo PULS, Laboratori Nazionali dell'INFN di Frascati, Frascati
Gruppo Nazionale di Struttura della Materia del CNR

1. - INTRODUCTION

The development of synchrotron radiation facilities has been growing fast in the last years both in Europe and in USA. It is crucial that the optical systems guarantee the maximum collection of radiation on the sample. In fact, the radiation emitted from the electrons orbiting in the storage ring must be focused onto the entrance slit of a monochromator with the proper f-number and the smallest image size. Since in the vacuum ultraviolet and in the soft X-ray regions every material is highly absorbing, the imaging systems are formed by one or several mirrors working at grazing incidence in order to take advantage of the higher reflectivity due to total reflection. However, at grazing incidence, aberrations are significant and reduce the intensity collected through the narrow slit of a monochromator.

A ray tracing program is the best way for studying the imaging properties of an optical system⁽¹⁾. The transversal dimensions of the radiation beam can be calculated at each point of the beam line, in particular in correspondence of the image, where the monochromator slit should be placed. By varying the parameters of the system it is possible to optimize the optical system. This work is easily achieved with a computer, but the optimization may require several hours of calculation.

In this and in the following reports we shall give the basic expressions for the ray tracing program used for the PULS facility constructed at the storage ring ADONE of the INFN National Laboratories. In the first report we shall develop the two-dimensional case, corresponding to the ray tracing in the meridian plane of the optical system⁽²⁾. In the other reports we shall concentrate on the three-dimensional case. The general expressions for the ray tracing are given in Sect. 2. In Sect. 3 we describe the imaging properties of the mirror by expanding the general relations of Sect. 2 in a power series of the divergence of the radiation emitted by the source. Explicit, analytical expressions are given. They are important for the optimization of the parameters of the system, since they can be handled easily. Finally, in Sect. 4 we shall apply the ray tracing to two illustrative examples.

2. - RAY TRACING IN THE MERIDIAN PLANE

The meridian plane of an optical system is the plane containing the central ray of the optical system and the normal to the mirror in its centre. We shall consider a mirror whose section in the meridian plane is an arc of circle of radius R . The case of a plane mirror can be derived in the limit of $R \rightarrow \infty$.

We choose a reference frame xz , where the x axis coincides with the central ray \mathcal{I}_0 moving from the source to the mirror along increasing values of x . The origin of the reference frame is on the surface of the mirror, which reflects towards positive values of z . The central ray, emitted from the point $S_0(-s, 0)$ of the source, is incident on the mirror in the origin with a tangent angle i_0 . The reflected central ray \mathcal{R}_0 forms an angle $r_0 = 2i_0$ with respect to the x axis (cfr. Fig. 1). From all the points $S(-s, \xi)$ of the source a small pencil of rays \mathcal{I} is emitted. The total divergence of the pencil, as well as the source dimensions are limited. Each ray is incident on the mirror with a

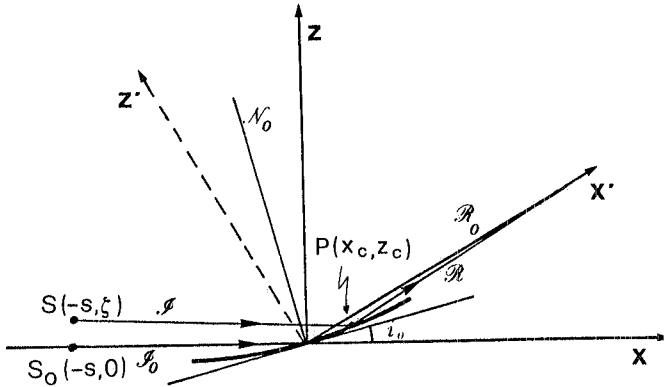


FIG. 1 - Coordinates and notations for the ray tracing on the meridian plane.

tangent angle i in the point $P(x_c, z_c)$. Our aim is to calculate the reflected rays \mathcal{R} and their intersections with a straight line perpendicular to \mathcal{R}_0 at the distance x' from the origin. This is easily done by rotating the coordinate axes around the origin by the angle r_0 , so that the new x axis (indicated as x') is coincident with the reflected central ray \mathcal{R}_0 . For a given value x' of the new abscissa, the new coordinate z' gives the image of the ray \mathcal{I} emitted from S . The transformed angular coefficient of the reflected ray corresponds to its angular divergence. We can express the above considerations in terms of cartesian coordinates and analytical geometry as follows:

$$\text{Incident ray } \mathcal{I}: \quad z = \text{tg } \theta (x+s) + \xi \quad (1)$$

$$\text{with } |\theta| \leq \theta_M \text{ and } |\xi| \leq \xi_M.$$

$$\text{Reflected ray } \mathcal{R}: \quad z = \text{tg } r (x-x_c) + z_c \quad (2)$$

$$\text{Equation of the mirror } \mathcal{C}: \quad (x-\alpha)^2 + (z-\beta)^2 = R^2. \quad (3)$$

$\alpha = -R \sin i_0$ and $\beta = R \cos i_0$ are the coordinates of the center of the mirror circle. The condition $\alpha^2 + \beta^2 - R^2 = 0$ guarantees that the circle passes through the origin.

The coordinates of $P(x_c, z_c)$ are obtained by intersecting \mathcal{I} with \mathcal{C} , i.e. by solving the system formed by Eqs. (1) and (3):

$$x_c = (1 + \operatorname{tg}^2 \theta)^{-1} \left[-b \pm \sqrt{b^2 - c(1 + \operatorname{tg}^2 \theta)} \right],$$

$$b = R \sin i_0 + \operatorname{tg} \theta (s \operatorname{tg} \theta + \zeta - R \cos i_0), \quad (4)$$

$$c = (s \operatorname{tg} \theta + \zeta) (s \operatorname{tg} \theta + \zeta - 2R \cos i_0).$$

Eq. (4) has two solutions, corresponding to the two intersections between a circumference and a straight line. We are interested in the point of intersection nearest to the coordinate origin, which is obtained by choosing the positive sign of Eq. (4). This choice is easily verified by letting θ and ζ converging to zero (condition for central ray) and obtaining $x_c = 0$. z_c is obtained by inserting x_c into Eq. (1):

$$z_c = \operatorname{tg} \theta (x_c + s) + \zeta. \quad (5)$$

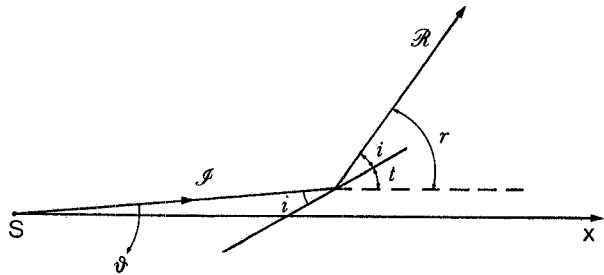
From geometrical considerations on the angles (see Fig. 2) we have $r = i + t$; $t = \theta + i$ and

$$r = 2t - \theta, \quad (6)$$

where t is the angle between the tangent to the circle in P and the x axis. By definition

$$\operatorname{tg} t = - \frac{x_c - a}{z_c - \beta}. \quad (7)$$

FIG. 2 - The relationships between angles.



From Eqs. (4), (5) and (6) we have the quantities x_c , z_c and $\operatorname{tg} r$ of Eq. (2), which defines the reflected ray as a function of the angular divergence θ of the incident ray and the displacement ζ of the source point with respect to the x axis. By rotating the reference frame around the origin, so that $x' \equiv \mathcal{R}_0$, the reflected rays have the equation:

$$z' = \operatorname{tg} r' (x' - x'_c) + z'_c, \quad (8)$$

where primed parameters r' , x'_c and z'_c are the transformed ones of the corresponding unprimed, i.e.:

$$\operatorname{tg} r' = \operatorname{tg} (r - r_0),$$

$$x'_c = \cos r_0 x_c + \sin r_0 z_c, \quad (9)$$

$$z'_c = -\sin r_0 x_c + \cos r_0 z_c.$$

Substituting the Eqs. (9) into Eq. (8) yields the following expression for z' :

$$z' = \operatorname{tg}(r-r_0) x' + \frac{\cos r}{\cos(r-r_0)} \left[(\operatorname{tg} \theta - \operatorname{tg} r) x_c + s \operatorname{tg} \theta + \zeta \right]. \quad (10)$$

Eq. (8) (or (10)) solves the ray tracing problem. At a given value of x' , a set of values of z' is obtained as a function of θ and ζ . We can check the correctness of Eqs. (4) to (9) by putting θ and ζ equal to zero. Then: from Eqs. (4) and (5) $x_c=0$ and $z_c=0$; from Eq. (7) $\operatorname{tg} t = \operatorname{tg} i_0$; from Eq. (6) $r = 2i_0 = r_0$. Thus x'_c, z'_c and $\operatorname{tg} r'$ are equal to zero and $z'=0$. The condition of central ray is verified.

If we have a system of mirrors, Eq. (8) (or (10)) can be used as the beam of rays incident on the next mirror. It is necessary to know the distance between the mirrors and the angle of incidence of the central ray onto each of them to perform a complete ray tracing calculation. Taking for each point of the source a set of θ values included in the range of allowed values, and moving the source point within the source itself, yields the image of the source in any position of the system. It is also possible to have an idea of the intensity distribution by counting the number of rays reaching the unit length $\Delta z'$ of the image as a function of θ and ζ , and by weighing each ray by its intensity factor.

3. - APPROXIMATE EXPRESSIONS

Usually, in the case of synchrotron radiation sources, the angular divergence θ of the beam is of the order of a few milliradians, and the distances between the source and the mirrors and between the mirrors themselves are large compared with the dimensions of the source (typically $\zeta/s \approx 10^{-3}-10^{-4}$). We can expand Eqs. (4-9) in power series of θ and ζ/s and obtain explicit expressions for the focussing properties of each mirror. We shall do this for the case $\zeta=0$ (central source) and we shall expand up to terms of θ^3 . The main equations of the previous section become:

$$z = \operatorname{tg} \theta (x + s) \approx \left(\theta + \frac{\theta^3}{3} \right) (x + s), \quad (1a)$$

$$x_c \approx \theta s \operatorname{ctg} i_0 \left[1 + a_1 \theta + a_2 \theta^2 \right], \quad (4a)$$

with

$$a_1 = \operatorname{ctg} i_0 - \frac{s}{2 R \sin^2 i_0 \cos i_0},$$

$$a_2 = \frac{1 + 2 \cos^2 i_0}{3 \sin^2 i_0} + \frac{s}{2 R \sin^3 i_0} \left(\frac{s}{R \sin i_0} - 3 \right),$$

and

$$z_c \approx s \theta + s \operatorname{ctg} i_0 \theta^2 + s \left(a_1 \operatorname{ctg} i_0 + \frac{1}{3} \right) \theta^3. \quad (5a)$$

The reflected rays are converging with a small angle $\theta' = r - r_0$ given by:

$$\operatorname{tg} \theta' \approx c_1 \theta + c_2 \theta^2 + c_3 \theta^3, \quad (11)$$

with

$$c_1 = \frac{2s}{R \sin i_0} - 1,$$

$$c_2 = \frac{2s}{R \sin i_0} \operatorname{ctg} i_0 \left(1 - \frac{s}{2R \sin i_0} \right),$$

$$c_3 = \frac{2s}{R \sin i_0} \left[\frac{3 + \sin^2 i_0}{3 \sin^2 i_0} - \frac{s}{2R \sin^3 i_0} (3 + 2 \sin^2 i_0) + \frac{s^2}{2R^2 \sin^4 i_0} (1 + 2 \sin^2 i_0) \right] - \frac{1}{3}.$$

Finally, the cross section of the reflected beam is given by:

$$z' \approx z_1 \theta + z_2 \theta^2 + z_3 \theta^3 \quad (12)$$

with

$$z_1 = \left(\frac{2s}{R \sin i_0} - 1 \right) x' - s,$$

$$z_2 = \frac{2s \operatorname{ctg} i_0}{R \sin i_0} \left[\left(1 - \frac{s}{2R \sin i_0} \right) x' - \frac{s}{2} \right],$$

$$z_3 = c_3 x' - s \left[\frac{1}{3} - (1 - 2 \operatorname{ctg}^2 i_0) \frac{s}{R \sin i_0} + (1 - \operatorname{ctg}^2 i_0) \frac{s^2}{R^2 \sin^2 i_0} \right].$$

Eqs. (11) and (12) give the most important results on the properties of a circular mirror. Let us examine Eq. (12). First, in the expansion the zero order term is missing, as it should, since $z'=0$ for $\theta=0$ (central ray condition). The focussing condition of a mirror requires that all the rays emitted from the source converge into the same point, independently from their angular divergence. In other words, all the coefficients of Eq. (12) must be zero for a certain value $x'=q$. This cannot be done for all of them simultaneously. Since the linear term $z_1 \theta$ gives the largest contribution to Eq. (12), the mirror equation is obtained by setting $z_1=0$. The corresponding value $x'=q$ gives the position of the image, according to:

$$\left(\frac{2s}{R \sin i_0} - 1 \right) q - s = 0 \Rightarrow \frac{1}{q} + \frac{1}{s} = \frac{1}{f}, \quad (13)$$

$$\frac{1}{f} = \frac{2}{R \sin i_0}. \quad (13a)$$

Eq. (13) is the equation of spherical mirrors, valid for every angle of incidence. In the case of oblique incidence, the focal length f depends on the angle of incidence. At normal incidence ($i_0=90^\circ$) Eq. (13) becomes the well known equation for spherical mirrors, with $f=R/2$. By introducing the magnification M of the mirror, $M=q/s$, and by using

Eq. (13), we can rewrite the linear terms of Eqs. (11) and (12) as

$$\theta' = \frac{\theta}{M} \quad (14a)$$

$$z' = (x' - q) \theta' \quad (14b)$$

Eqs. (14a) and (14b) have a simple interpretation. At any angle of incidence, a mirror behaves as in the case of normal incidence and Gauss optics: the ratio between the divergences of the beams emitted from the source and converging to the image, is given by the magnification of the mirror. The width of the reflected beam is given by its convergence at the image times its distance from the imaging point. Thus, the major features of the properties of light beams (beam size and divergence) are described by the first order formulae, that are the same as those of Gauss optics, with the exception of the focal length, which changes with the angle of incidence.

The second and higher order terms give the deviations from perfect imaging and correspond to the mirror aberrations. The coefficient of the square term of Eq. (11) is given by:

$$c_2 = \frac{s \operatorname{ctg} i_0}{f} \left(1 - \frac{s}{4f}\right) = \frac{\operatorname{ctg} i_0}{4M^2} (M+1)(3M-1). \quad (15)$$

For not too small i_0 , this equation is of the order of a few units and so the second term is of the order of 10^{-2} with respect to the first order term. Also the higher order terms in z' are much smaller than z_1 and they can be neglected safely, except in the image position, where the linear term is zero. Thus, this term gives the aberration of the mirror. For $x'=q$, z_2 is

$$z_2 = \frac{3 s \operatorname{ctg} i_0}{4 M} (M^2 - 1). \quad (16)$$

In the position of the image all the aberration extends on the same side of the central ray, with a distribution of rays decreasing fast moving from the central ray according to:

$$\frac{d\theta}{dz'} = \frac{1}{2} \sqrt{\frac{4M}{3s \operatorname{ctg} i_0 (M^2 - 1)}} \frac{1}{\sqrt{z'}} \quad (17)$$

Eq. (16) is the same as that reported by Kirkpatrick and Baez⁽³⁾, who derived it for X-ray mirrors operating at very small tangent angles. In the case of $M=1$, the second order aberration term becomes zero and one needs higher order terms. This result was obtained previously by Namioka⁽⁴⁾ for the imaging properties of a spherical concave grating on the Rowland circle - the zero order diffraction term corresponds to specular reflection in the case of gratings.

In the case of $M=1$, the third order term

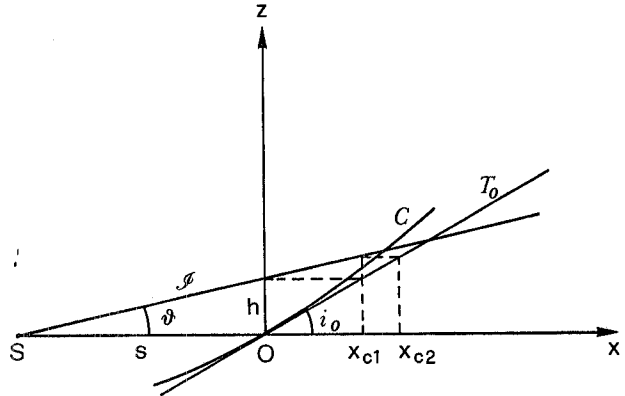
$$z_3 \theta^3 = \frac{s \theta^3 (M+1)}{4M^2 \sin^2 i_0} \left[\left(\frac{1}{2} + \cos^2 i_0 \right) (M-1)^2 - 2M \cos^2 i_0 \right] = -s \theta^3 \operatorname{ctg}^2 i_0, \quad (18)$$

must be considered. This is a very small quantity and it is symmetric with respect to the central ray. It is worth noting that both z_2 and z_3 depend directly on $\operatorname{ctg} i_0$: as expected, at normal incidence this coefficient is zero and the circular mirror is aberration free, a well known result of Gauss optics and paraxial rays. Instead, the aberration terms increase for more and more grazing incidence.

A few comments about Eq. (4a) giving x_c . This equation has a very simple geometrical interpretation. (cfr. Fig. 3).

$$x_c = s \theta \operatorname{ctg} i_o + s \theta^2 \operatorname{ctg}^2 i_o - \frac{\theta^2 s^2 \operatorname{ctg} i_o}{2R \sin^2 i_o \cos i_o} + \dots \quad (19)$$

FIG. 3 - Derivation of the coordinate x_c from simple geometrical approximations.



The first term corresponds to the abscissa of the intersection as if the height of the beam is calculated at the centre of the mirror surface and the mirror is a plane one: $h=s \theta \Rightarrow x_c(1) = h \operatorname{ctg} i_o = s \theta \operatorname{ctg} i_o$. The first part of the quadratic terms, $s \theta^2 \operatorname{ctg}^2 i_o$, corresponds to the additional length of the mirror because the beam is diverging from 0 to $x_c(1)$. In fact it can be rewritten as $x_c(1) \theta \operatorname{ctg} i_o$. This term adds to $x_c(1)$ for positive θ and subtracts for negative θ , and thus it must be quadratic (note that $x_c(1)$ changes sign with θ). Finally, the second part of the quadratic term $(\theta^2 s^2 \operatorname{ctg} i_o)/(2R \sin^2 i_o \cos i_o)$ is due to the curvature of the mirror.

4. - ILLUSTRATIVE EXAMPLE

We consider now two examples related with the PULS facility corresponding respectively to S_1 , the first mirror of the vacuum ultraviolet beam line, and to S_2 , the first mirror of the grasshopper beam line. The parameters of these two mirrors are reported in Table I, from which the choice of these two examples becomes evident. S_1 works at a not too small grazing incidence with magnification $M=2$. S_2 works at a rather small angle of

TABLE I - Parameters of the mirrors S_1 and S_2 .

| | S_1 | S_2 |
|-------------------|--------|--------|
| i_o | 13.9° | 4° |
| s(m) | 6.32 | 8.50 |
| R(m) | 35.078 | 121.85 |
| q(m) | 12.64 | 8.50 |
| θ_M (mrad) | 3 | 1 |
| M | 2 | 1 |

incidence, in which case the aberrations should be large; but it has a one-to-one magnification, so that only third and higher order terms contribute to the aberrations.

The results of the ray tracing calculation are shown in Fig. 4 for the mirror S_1 and in Fig. 5 for the mirror S_2 . In the two figures a few rays, corresponding to some values of θ , are traced from 0.5 m before to 0.5 m after the focal points of the mirrors. Each ray is labelled by the corresponding value of θ , expressed in mrad, the ray $\theta=0$

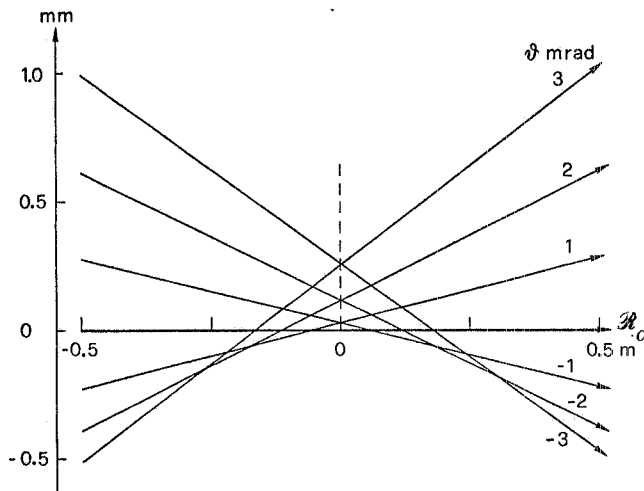
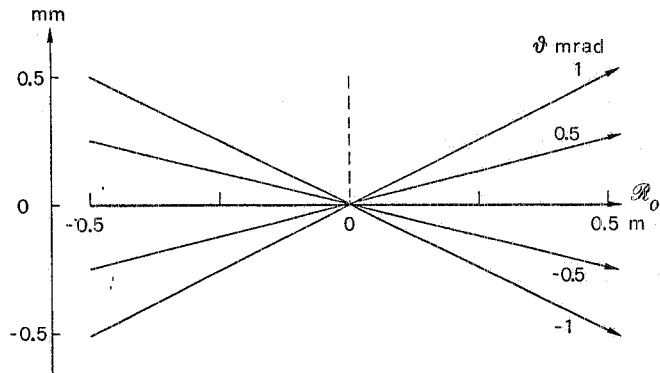


FIG. 4 - Ray tracing results for the mirror S_1 near the image at $q=12.64$ m. A few rays, each of them labelled with the corresponding value of θ , have been traced from $(q-0.5)$ m to $(q+0.5)$ m. Note that the abscissa scale is in meters, while the vertical scale is in mm.

FIG. 5 - Ray tracing results for the mirror S_2 near the image at $q=8.50$ m. A few rays, each of them labelled with the corresponding value of θ , have been traced from $(q-0.5)$ m to $(q+0.5)$ m. Note that the abscissa scale is in meters, while the vertical scale is in mm.



being the central ray. Note that the vertical scales are in mm, while the horizontal ones are in m. A significant difference between the two figures can be noticed. For S_1 , at the image, all the rays are above the central ray, giving an aberration approximately 0.26 mm wide. Instead, in the case of S_2 , all the rays are intersecting symmetrically with respect to the central ray, with an almost aberration-free image, as the result of $M=1$. In Table II we give some of the parameters calculated for the two mirrors with the ray tracing procedure illustrated in Sect. 2. These values are then compared with the approximate expressions given in Sect. 3, where terms up to θ^3 have been included.

From Table II, we see that the approximate relations derived in Sect. 3 are accurate enough already in the first order terms for most practical purposes, such as the dimensions of the reflection surface. In fact, the actual reflecting surface must be framed by several mm of mirror for bracketing the mirror to its holder and for the positioning in the beam line and this is by no means larger than the correction of the second order term.

More interesting is the case of the image. For S_1 the $z_2\theta^2$ term already gives the significant information on the spreading of the aberration. The dimensions of the image of the actual, finite source are given by its size magnified by the mirror (2 mm for S_1 , supposing an electron beam of 1 mm), with some blurring extending 0.26 mm on one side of the image due to the aberrations. In the case of S_2 this blurring is practically missing. Scattering from dust or construction imperfections caused by the accuracy in following the theoretical profile as well as by polishing the surface of the mirror, are more important in smearing the image produced by S_2 than the aberrations.

TABLE II - Numerical results of the ray tracing for the mirrors S_1 and S_2 . In the first column we indicate the quantities that have been calculated at the values of θ given in column 2. In the third column we give the numerical results obtained from the ray tracing program described in Sect. 2. In columns four, five and six we list the numerical results obtained by using the approximate expressions of Sect. 3, with the single contributions from the different powers of θ given separately as indicated. The total is reported in the last column.

| | | θ | ray tr. | Approximate expressions | | | |
|-------|-----------------|----------|-----------|-------------------------|------------|------------|---------|
| | | | | θ | θ^2 | θ^3 | Total |
| S_1 | x_c (mm) | +3 | 77.174 | 76.614 | 0.559 | 0.001 | 77.174 |
| | | -3 | -76.059 | -76.614 | 0.559 | -0.001 | -76.059 |
| | θ (mrad) | ± 3 | ± 1.5 | | | | |
| | z' (mm) | +3 | 0.2573 | - | 0.2586 | -0.0013 | 0.2573 |
| -3 | | 0.2598 | - | 0.2586 | 0.0013 | 0.2599 | |
| S_2 | x_c (mm) | +1 | 122.42 | 121.56 | 0.865 | | 122.42 |
| | | -1 | -120.69 | -121.56 | 0.865 | | -120.69 |
| | θ (mrad) | ± 1 | ± 1 | | | | |
| | z' (mm) | +1 | -0.0018 | - | - | -0.0017 | -0.0017 |
| -1 | | 0.0017 | - | - | +0.0017 | +0.0017 | |

ACKNOWLEDGEMENTS

We acknowledge Prof. F. Bassani, Director of PULS, and Prof. R. Scrimaglio, Director of the LNF, for their interest in this work. We thank also Dr. A. Savoia for several stimulating discussions. PULS is a research program run jointly by the Italian National Research Council and the Italian National Institution for Nuclear Physics.

REFERENCES

- (1) O.N. Stavroudis, *The Optics of Rays, Wavefronts, and Caustics*, (Academic Press, New York 1972).
- (2) A. Balzarotti, A. Bianconi, E. Burattini, and M. Piacentini, LNF Report 74/32(R) (1974).
- (3) P. Kirkpatrick and A.V. Baez, *J.O.S.A.* **38**, 766 (1948).
- (4) T. Namioka, *J.O.S.A.* **49**, 446 (1959).